AIChE

Plasmid-Encoded Protein Attenuates *Escherichia coli* Swimming Velocity and Cell Growth, not Reprogrammed Regulatory Functions

Chelsea Virgile
Institute for Bioscience and Biotechnology Research, MD, 20742
Fischell Dept. of Bioengineering, University of Maryland, MD, 20742

Pricila Hauk
Institute for Bioscience and Biotechnology Research, MD, 20742
Fischell Dept. of Bioengineering, University of Maryland, MD, 20742

Hsuan-Chen Wu
Dept. of Biochemical Science and Technology, National Taiwan University, Taipei City, Taiwan

William E. Bentley
Institute for Bioscience and Biotechnology Research, MD, 20742
Fischell Dept. of Bioengineering, University of Maryland, MD, 20742

DOI 10.1002/btpr.2778
Published online February 15, 2019 in Wiley Online Library (wileyonlinelibrary.com)

In addition to engineering new pathways for synthesis, synthetic biologists rewire cells to carry out "programmable" functions, an example being the creation of wound-healing probiotics. Engineering regulatory circuits and synthetic machinery, however, can be deleterious to cell function, particularly if the "metabolic burden" is significant. Here, a synthetic regulatory circuit previously constructed to direct Escherichia *coli to swim toward hydrogen peroxide, a signal of wound generation, was shown to work even with coexpression of antibiotic resistance genes and genes associated with lactose utilization. We found, however, that cotransformation with a second vector constitutively expressing GFP (as a marker) and additionally conferring resistance to kanamycin and tetracycline resulted in slower velocity (Δ~6 μm/s) and dramatically reduced growth rate (Δ > 50%). The additional vector did not, however, alter the run-and-tumble ratio or directional characteristics of H_2O_2–dependent motility. The main impact of this additional burden was limited to slowing cell velocity and growth, suggesting that reprogrammed cell motility by minimally altering native regulatory circuits can be maintained even when extraneous burden is placed on the host cell.* © 2019 American Institute of Chemical Engineers *Biotechnol. Prog.*, 35: e2778, 2019.
Keywords: CheZ, metabolic burden, constitutive fluorescence, motility, synthetic biology

Introduction

In our previous work,[1] *Escherichia coli* were engineered to respond and swim toward hydrogen peroxide, a non-native and potentially toxic signal, using the *oxyR/S* gene-promoter for hydrogen peroxide signaling. Specifically, motility regulator, CheZ, was induced using hydrogen peroxide to guide swimming in *cheZ* null mutants. These studies were motivated by the desire to create "smart" probiotics,[2–8] including those that swim to specific biomarkers,[9–13] providing spatial control of the delivery of their therapeutic payload. Here, in the presence of elevated H_2O_2 levels, transcriptional regulator, OxyR, undergoes a structural conformation change which results in subsequent activation of transcription of many promoters involved in oxidative stress, including *oxyS* [14,15]. Thus, our minimal circuit results in the expression of CheZ *via oxyS* that, in turn, reconstitutes the CheZ/CheY regulatory network so that the *ΔcheZ* cells can swim normally. Cells swimming in the presence of H_2O_2 and that are immotile in locales devoid of H_2O_2, over time accumulate in regions of high H_2O_2 in a process of pseudotaxis.[1] We were interested in understanding whether cells burdened with extraneous gene expression would retain wild-type motility. Engineered probiotics that have impaired native function owing to over engineered genetic circuitry and heterologous gene expression are less likely to perform as designed.[16,17]

We characterized cell growth and motility using the previous 1-plasmid motility vector (pHW02) and, in addition to expressing CheZ, this vector confers (i) resistance to ampicillin (β-lactamase expression), (ii) utilization of lactose (*lacZ*, *lacY*, *lacA*, expression), and (iii) copy number maintenance by expression of *repE* (mini-F plasmid, 1–2 copies per cell). We then repeated these studies using two plasmids (pHW02 & pET200-t5-eGFP), the latter conferring GFP visualization *via* constitutive (uninduced) T5 promoter control, and additional

Additional supporting information may be found online in the Supporting Information section at the end of the article.

Correspondence concerning this article should be addressed to W. E. Bentley at bentley@umd.edu

antibiotic resistance using a ColE1 origin of replication (~20 copies per cell).

Results

Previous qPCR experiments using pHW02 and varying concentrations of H_2O_2 had shown increased *cheZ* mRNA within 5–10 min, especially when H_2O_2 concentrations were above 12.5 μM. Moreover, we observed a dose dependent effect between 12.5 and 200 μM.[1] An identical dose dependent response is recapitulated here at 15 min postinduction (Figure 1a). We further characterized CheZ levels using Western blot and found significant differences between the 1-plasmid versus 2-plasmid systems (plasmid maps are provided in Supporting Information). Readily visible bands were observed for the 1-plasmid system in both 15 and 60 min samples, particularly at higher doses of H_2O_2, as expected (Figure 1b). Only faint CheZ bands were observed for the 2-plasmid system after 60 min of induction, however. This suggests that addition of the second plasmid, with constitutive expression of GFP, attenuated CheZ expression.

While many previous studies have examined the effects of plasmid-encoded gene overexpression[18–21] on cell growth and protein expression, there was no way to *a priori* to predict whether these "metabolic burden" effects would alter the H_2O_2 inducer consumption rates of our system or the subsequently actuated cell motility. When we induced these cells at the higher of two cell densities (OD 0.4 vs. OD 0.1), in all cases (1- & 2-plasmid systems) all of the H_2O_2 (50 and 100 μM) was consumed within 5 min (Figure 1c). These data coincide with hydrogen peroxide induced expression of CheZ. The raw spectrophotometric data were converted to concentration in Figure 1c. Interestingly, in all cases with cells induced at the lower cell density (OD 0.1), there was H_2O_2 remaining (Figure 1c) at the end of the cultures. Also, the level of H_2O_2 remaining was higher for the 2-plasmid system, indicating that H_2O_2 uptake was somewhat attenuated in these cells.

As expected, we observed significant differences in growth rate between systems (Figure 2a). The presence of the second vector decreased cell growth rate by over half. In the latter exponential phase, (Figure 2a [left]), cells with an empty vector were induced with 100 μM H_2O_2 and the cell growth rates were determined (Figure 2b). The WT and HCW01 (*ΔcheZ*) cells grew identically. In the cases when the second vector was added, the growth rate had dropped precipitously. Results suggest there was no difference in growth due to the *cheZ* deletion, rather a significant change due to the second plasmid. In Figure 2a (right), hosts transformed with the *cheZ* plasmid with *oxyRS* control (pHW02) were also transformed with the

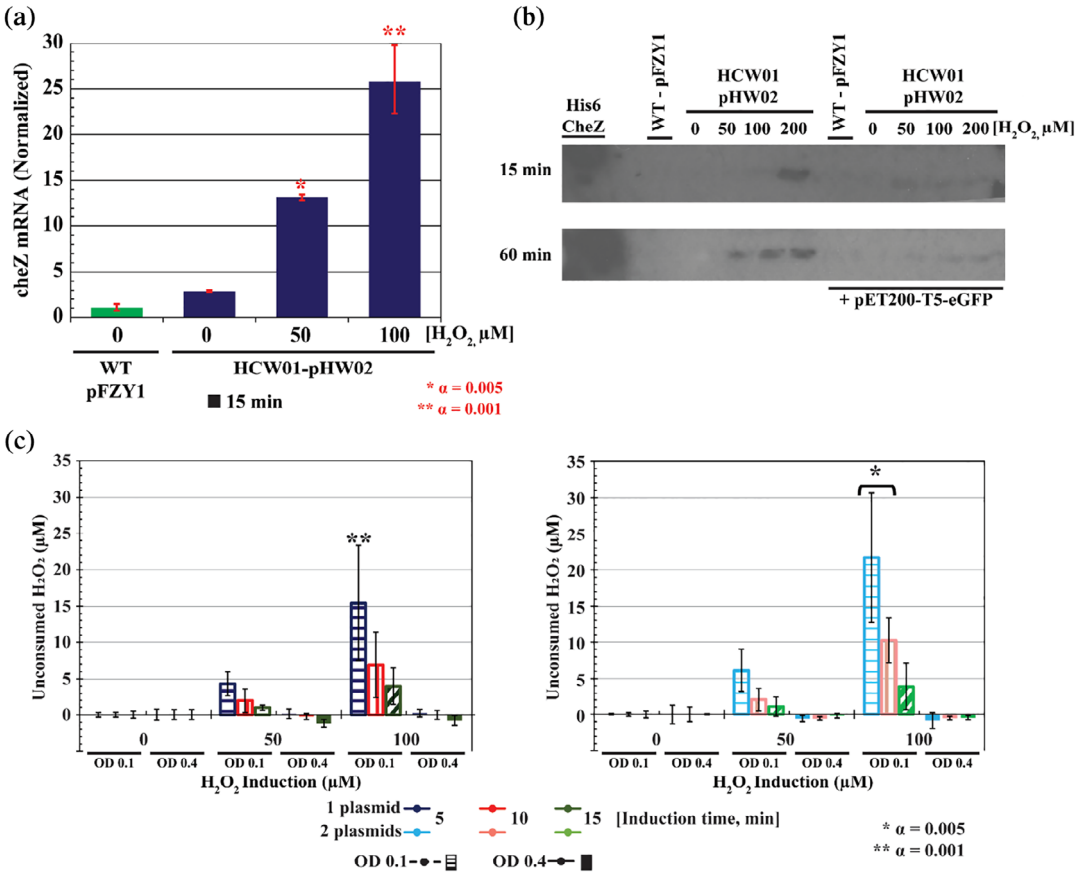

Figure 1. Hydrogen peroxide-induced expression of motility regulator, CheZ. (a) qPCR analysis of *cheZ* mRNA for 1-plasmid system using *E. coli* HCW01 (*cheZ* mutant) cells—15 min sample time. (b) Western blots showing CheZ levels post-induction for 1-plasmid & 2-plasmid systems. Hydrogen peroxide induction was for 15 and 60 min. Cultures with overexpressed His_6-CheZ and the empty plasmid (W3110-pFZY1) were included as controls. (c) Hydrogen peroxide remaining after cells were induced at different optical densities (indicated), with indicated levels of H_2O_2 and at indicated sample times. A 1-plasmid system not expressing CheZ (HCW01-pFZY1) is at the left and the 2-plasmid system with CheZ expression is at the right (HCW01-pHW02). Tukey–Kramer ANOVA and multiple comparisons analyses were performed with * α = 0.005. * indicates the samples differed significantly from all samples.

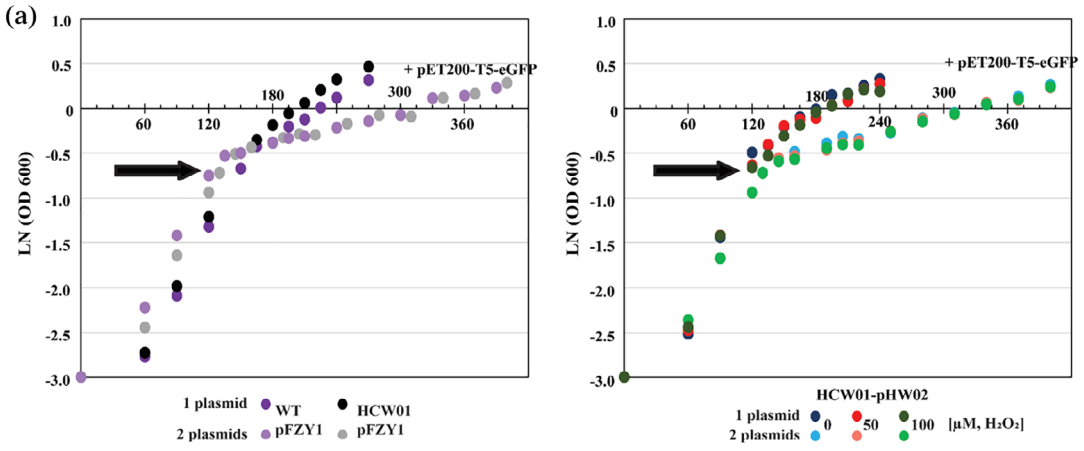

(b)

H_2O_2 (μM)		LINEST ± Error (hr^{-1})	
1 plasmid	WT	0.48 ± 0.03	
	HCW01	0.50 ± 0.03	
2 plasmids	WT	0.20 ± 0.01	p < 0.0001
	HCW01	0.19 ± 0.01	p < 0.0001

H_2O_2 (μM)		LINEST ± Error (hr^{-1})	
1 plasmid	0	0.42 ± 0.03	
	50	0.42 ± 0.04	
	100	0.45 ± 0.04	
2 plasmids	0	0.20 ± 0.01	p < 0.0001
	50	0.20 ± 0.01	p < 0.0001
	100	0.20 ± 0.01	p < 0.0001

Figure 2. Attenuated growth of cell cultures expressing CheZ with an additional GFP reporter plasmid after induction with hydrogen peroxide. (a) (left) Cultures without exogenous CheZ expression but with and without supplemental GFP expression. Wild type *E. coli* W3110 (WT-pFZY1) and HCW01-pFZY1 (*cheZ* mutant) were grown with and without pET200-eGFP. The presence of the second vector significantly reduced cell growth but the addition of H_2O_2 had no additional effect. Also, growth differences due to deletion of *cheZ* were negligible. (right) The same host, *E. coli* HCW01 (*ΔcheZ*) with hydrogen peroxide induced CheZ (HCW01-pHW02) grew more slowly with the GFP vector. H_2O_2 level and CheA induction had no effect. The black arrows indicate the induction times intiated at OD_{600} 0.5. After induction, bacterial cultures were shaken at 24°C and sampled every 15 min for 2 h (one plasmid) or 4 h (2 plasmids). (b) Tables indicate calculated specific growth rates postinduction using ANCOVA linear regression analyses (Prism). For data analysis, technical and biological triplicate data were obtained.

second reporter plasmid. Here, the addition of hydrogen peroxide had little or no apparent effect in the absence of the second plasmid. Similarly, with the second plasmid present the depression in cell growth in the presence of hydrogen peroxide did not appear to be a function of hydrogen peroxide concentration (Figure 2b). That is, the apparent induction of CheZ, in no case, appeared to exert an additional effect on cell growth. Moreover, because there was no apparent difference between those with and without hydrogen peroxide, the addition of hydrogen peroxide (e.g., 100 μM) in the presence of the second vector was not responsible for altering growth. These results were remarkably consistent; the presence of the second vector clearly reduced cell growth relative to controls during the late exponential phase.

Having significantly altered growth patterns, we forged ahead and analyzed bacterial movement using a 2D phase contrast microscopy system[22,23] and cell motility videos. We used 5 s trajectories and Tumblescore[22] for analysis of velocity and other motility parameters. In Figure 3a, a few trajectories are depicted from representative traces; that is, a black trace is produced as a cell moves from the beginning of its trajectory to its end at the end of a video trace. Similarities between the mutant and engineered cells without H_2O_2 are striking, as are the wild-type cells without H_2O_2 and engineered cells with H_2O_2, regardless of metabolic burden. By inspection, there were no obvious differences between the 1- and 2-plasmid trajectories. In Figure 3b, Rose plots are depicted wherein many traces are superimposed with their initial points set at the origin of the coordinate axes. We found increased trace distance with increased H_2O_2 for both systems. We also noticed that trajectories were observed in every direction, as expected. However, when comparing the 1- versus 2-plasmid systems, the 2-plasmid system appeared to have slightly shorter path lengths.

To more directly quantify the phenotypic responses we performed computational analyses[22] of the motility videos. In Figure 4a,b and consistent with our previous study, the velocity in the *cheZ* mutants was reduced. For both the 1- and 2-plasmid systems, the addition of hydrogen peroxide and induced CheZ appeared to fully restore velocity to that of the wild-type strain transformed with an empty vector (pFZY1). In addition, a consistent reduction in velocity was observed for the *cheZ* mutant cases due to the presence of the second plasmid expressing GFP. That is, while the expression of CheZ appeared to fully restore velocity to the wild-type transformed control, that control (and all other 2-plasmid system cases) exhibited reduced velocity. This reduction directly links the metabolic burden previously observed for cell growth to cell motility.

Another quantity used to characterize swimming is the net angle change as a cell moves from frame to frame. For 5 s trajectories, the percentage of trajectories that exhibited a net

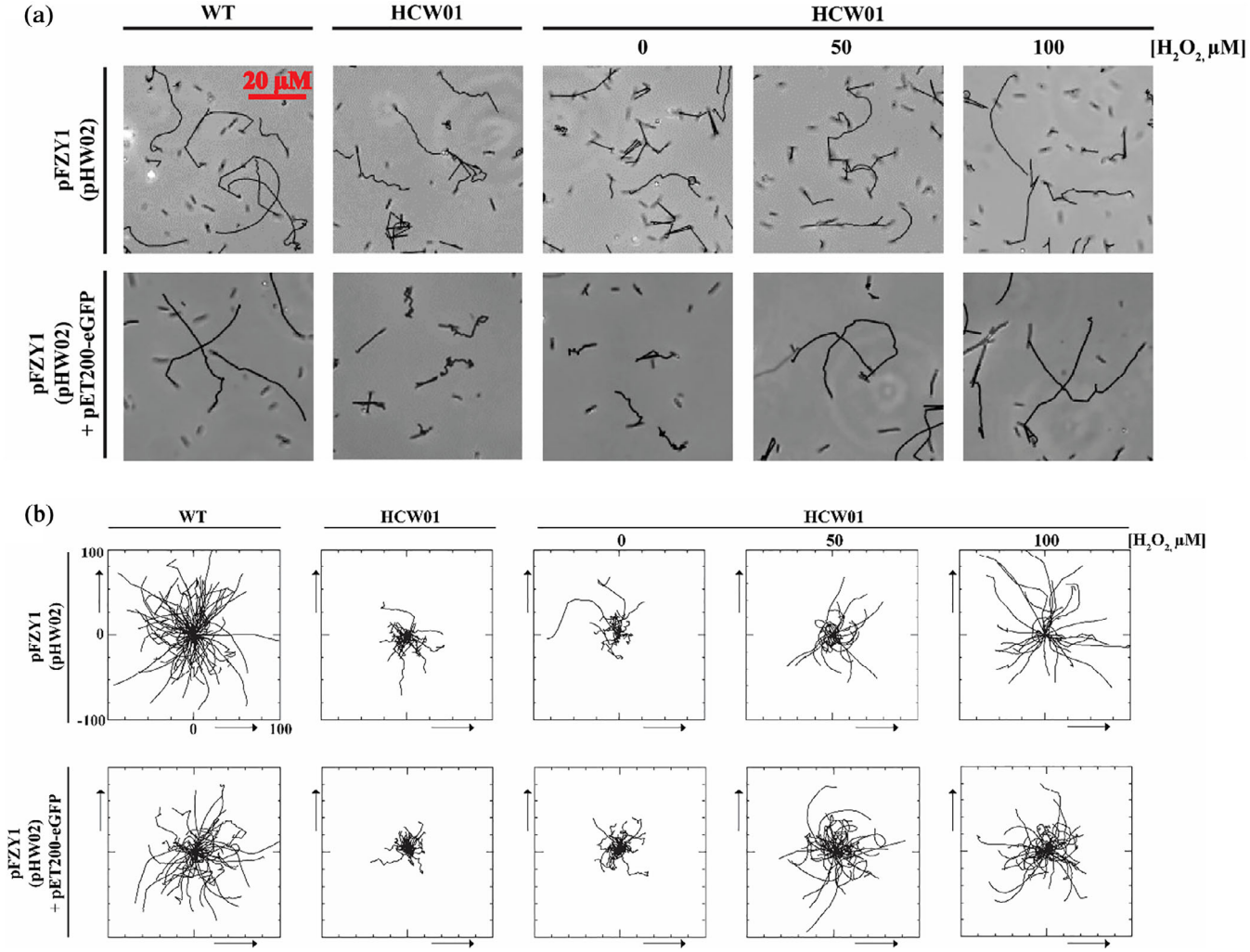

Figure 3. Motility trajectories following hydrogen peroxide-induced CheZ. (a) Phase contrast trajectory images. 5 s trajectories of WT-pFZY1, HCW01-pFZY1, and HCW01-pHW02 (0–100 μM hydrogen peroxide) ± pET200-eGFP were mapped. (b) Rose graphs of trajectories. 5 s trajectories are displayed from each trajectory's origin to visualize the path lengths (axes span 200 μm) and angle changes with and without the pET200-eGFP plasmid.

angle change of <1 rad/s and > 1 rad/s were classified as "running" or "tumbling," respectively.[24] Interestingly, we found that despite the statistically significant differences in velocity, there was no significant difference in the percentage of running (Figure 4c,d) among the H_2O_2 induced 1- and 2-plasmid systems. Further, WT-pFZY1 and H_2O_2-induced HCW01-pHW02 running times were calculated to be ~40–50%; the H_2O_2-induced bacteria had recovered the native run versus tumble percentages. As expected, however, the HCW01-pFZY1 and uninduced HCW01-pHW02 running times were significantly reduced.

Finally, we calculated the ratio of total path length to Euclidean distance (Figure 4e,f,g). This is the sum of all discrete distances traveled divided by the net distance from the beginning to end of a trajectory (Figure 4e). As expected, bacteria without *cheZ* in both systems exhibited a higher ratio than the wild type. Also, they appeared to exhibit fairly uniform distributions (as indicated by reduced breadth of the quartiles in the box and whisker plots). Interestingly, the presence of the second vector seemed to narrow the distribution in this ratio among all cases, although we did not statistically validate this observation. More importantly, transforming cells with the *oxyS-cheZ* vector broadened the distribution, while subsequent induction with hydrogen peroxide appeared to bring levels back to the WT levels and also tighten the distribution. Specifically, when we reintroduced *cheZ* to both 1- and 2-plasmid systems, the ratio dropped back to the WT-pFZY1 level in the 1-plasmid system, but increased further in the 2-plasmid system. Then, however, when we induced these cells, in all cases the ratio was restored to the WT-pFZY1 levels (or even lower) and with less deviation. The apparent increase in distribution that accompanied introduction of the second plasmid was somewhat perplexing. We have no hypothesis for its occurrence.

Here, we engineered a synthetic H_2O_2-responsive promoter system that was meant to restore swimming characteristics in *cheZ* mutants to the wildtype isogenic host. This was successful. That is, we used a single cell-based analytical method to characterize the system that enables *E. coli* to sense H_2O_2 and respond in highly-controlled and defined manner. We measured cell growth rate during the late exponential phase, velocity, the percentage of run versus tumble, and the ratio of path length to Euclidean distance. Importantly, the genetic circuit alone, when introduced on a 1-plasmid vector with F′ origin of replication and when actuated, exhibited no influence on cell growth and was observed to fully restore all measures characterizing swimming. Conversely, the added influence of a second, medium copy number plasmid (ColE1 origin) that

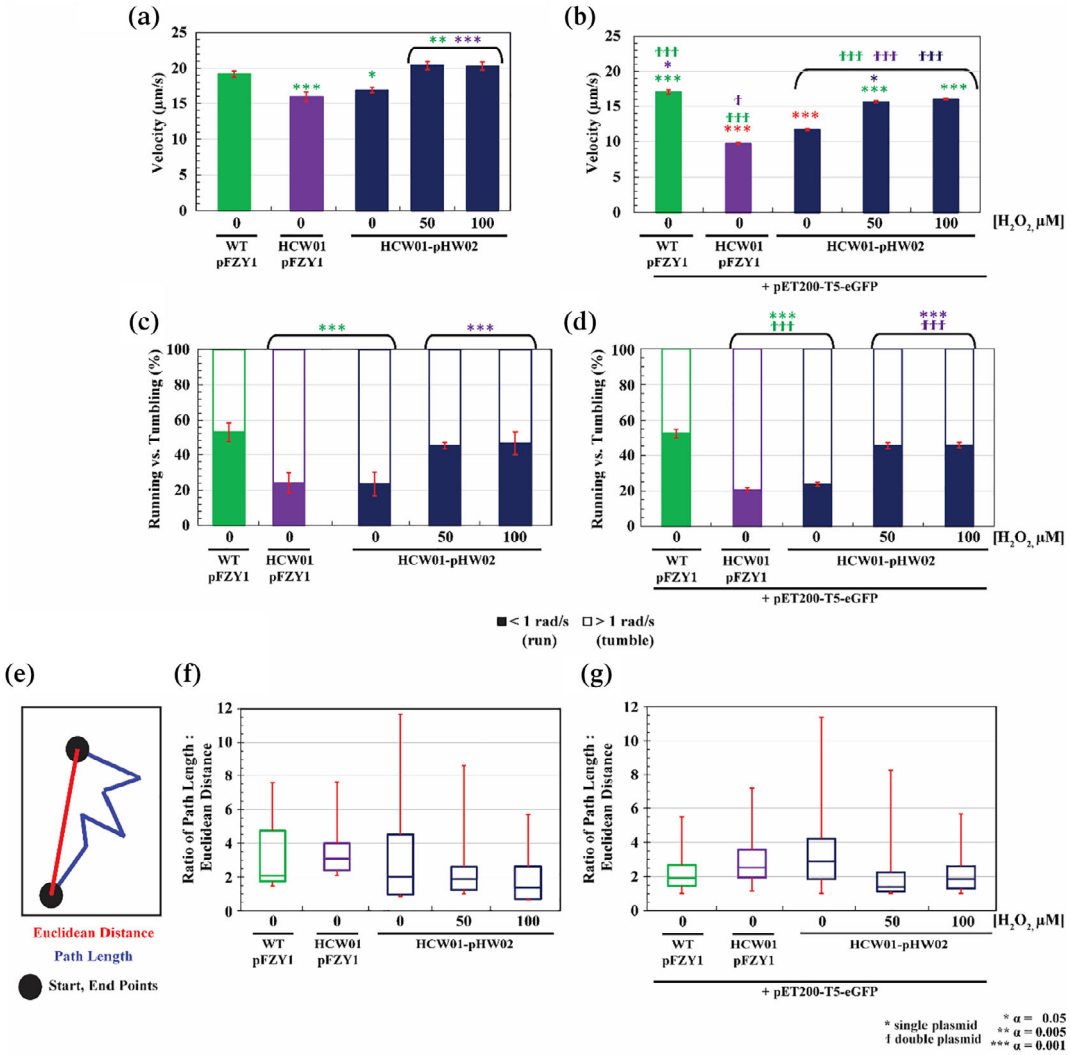

Figure 4. Motility characteristics upon hydrogen peroxide-induced CheZ. (a and b) Average velocities. The average velocities of the control bacteria (WT-pFZY1, HCW01-pFZY1) vs.the engineered bacteria (HCW01-pHW02; 0–200 μM hydrogen peroxide) without (left) and with pET200-eGFP *(right)*. (c and d) Fraction of running vs. tumbling (angular velocities) within the first 5 s of each trajectory. Calculations are based on identifying a tumble as movement under 1 rad/s based on angle change estimates. The percentage of trajectories (based on the initial 5 s trajectories of all bacteria) that were "running" vs. "tumbling" based on the time it took to move either <1 rad/s or > 1 rad/s, respectively. The error bars are the calculated standard error. (e–g) Ratio of path length: Euclidean distance. (e) The total distance traveled (path length, blue line) vs. displacement (Euclidean distance, red line) is demonstrated in this figure. The values were calculated based on the initial 5 s trajectories of all bacteria and plotted as box and whisker (f,g) to determine if there were significant differences in the averaged length and the distributions between the 1-plasmid and 2-plasmid systems. The boxes outline the lower quartile (lower box, Q1), median (the divisive line inside the box), and upper quartile (upper box, Q3). The whiskers indicate the highest and lowest observations (red lines). Tukey–Kramer ANOVA and multiple comparisons analyses were performed with α = 0.05–0.001. * indicates the samples differed significantly from the one plasmid system. † indicates the samples differed significantly from the two plasmid systems. For data analysis, technical duplicate and biological triplicate data were obtained.

provides T5-promoter driven constitutive (e.g., uninduced) GFP expression and an additional two antibiotic resistance genes dramatically reduced cell growth with our without the presence of hydrogen peroxide. It also attenuated swimming velocity. Our hypothesis is that the extra burden placed on the cell by the expression of GFP and other proteins may in effect, have resulted in moving beyond a "tipping point" above which cells grow more slowly, swim more slowly, and otherwise act differently. That the second vector was a medium copy number vector added on top of the single copy number vector is also important, as it is the additional expressed protein enabled by the multicopy plasmid that is the principle cause of the metabolic burden (and not the copy number per se[18]).

We note that GFP is commonly used by researchers to quantify gene expression and without apparent influence, but we found it and the expression of an additional two antibiotic resistance genes can reduce cell growth rate when introduced in the seemingly innocuous manner shown here (e.g., as expressed on a second, multicopy number plasmid). Further, GFP is also widely used when conducting motility experiments[25,26] and here, when presented to cells as an independent second-plasmid marker, its presence was seen to significantly reduce velocity. That said, neither GFP nor the second vector appeared to affect the *cheZ* network. It is well known that flagella require ATP and ATPases to rotate[27,28]; our results suggest that the 2-plasmid bacteria are ladened with an energetic metabolic burden that serves to reduce bacterial growth rate

and swimming velocity. Despite this burden, the engineered bacteria were observed to quickly consume the majority of the H_2O_2 and returned to near WT running. That is, irrespective of the metabolic load that might accompany engineered signal recognition as well as signal-actuated synthesis of a therapeutic, the motility circuit seemed to be robust—enabling further use in probiotic designs. In addition to providing additional insight on the metabolic effects of recombinant protein expression in *E. coli*, we believe the synthetic biology framework and tracking analysis in this work helps to quantify bacterial motility and can help determine the optimal designs for eventual deployment of "smart" probiotic systems.

Materials and Methods

System assembly and growth conditions

The genetic constructs developed in this study were assembled by Dr. Hsuan-Chen Wu of National Taiwan University using standard synthetic biology protocols.[29] Synthesized strains are W3110-pFZY1 (WT-pFZY1), W3110-ΔCheZ-pFZY1 (HCW01-pFZY1), and W3110-ΔCheZ-pFZY1-OxyR-pOxyS-CheZ (HCW01-pHW02; ampicillin resistance, Sigma-Aldrich, St. Louis, MO). The strains were then transformed with pET200-eGFP (kanamycin resistance, Sigma-Aldrich, St. Louis, MO). For all overnight inoculations, bacteria were grown from glycerol frozen stock; all morning reinoculations were diluted to OD_{600} 0.05. All bacterial cells were maintained in LB media (Fisher Scientific, Pittsburgh, PA) with appropriate antibiotic(s) supplemented in all experiments and incubated at 37°C in a shaker at 250 rpm for all motility experiments.

Bacterial growth curves

E. coli containing either one or two plasmids were inoculated into 25 mL of LB in 125 mL flasks. Culture flasks were shaken at 37°C and sampled every 30 min until OD_{600} ~0.5 was achieved. After induction, flasks were shaken at 24°C and sampled every 15 min for 2 h (one plasmid) or 4 h (two plasmids). For data analysis, technical, and biological triplicate data were obtained. ANCOVA linear regression analysis was performed using Prism.

Hydrogen peroxide consumption

E. coli containing either one or two plasmids were inoculated into 10 mL of LB in 50 mL flasks, and shaken at 37°C until OD_{600} ~0.5 was achieved. Cells were pelleted and resuspended in fresh LB at OD_{600} 0.1 and 0.4. The bacteria were induced with 0, 50, and 100 μM H_2O_2 in clear 96-well plates (total volume—200 μL) at 24°C, 250 rpm for 5–15 min. All samples were assayed for H_2O_2 with standards using the Quantitative Peroxide Assay Kit (Pierce, Thermo Fisher Scientific). A SpectraMax M2 plate reader (Molecular Devices) was used to read colorimetric absorbance (595 nm) to calculate the amount of unconsumed H_2O_2. For data analysis, technical, and biological triplet data were obtained.

cheZ *qPCR and CheZ Total protein quantification*

E. coli containing either one or two plasmids were grown overnight, reinoculated into 25 mL of LB in 125 mL flasks, and shaken at 37°C until OD_{600} of 0.5 was achieved. Cells were induced with 0–200 μM H_2O_2 at 24°C, 250 rpm for 15 and 60 min and then centrifuged at 4°C, 12,000 rcf for 10 min. Bacterial pellets were resuspended with 200 μL BugBuster (BugBuster HT, EMD Millipore) and protease inhibitor (HALT Protease Inhibitor Cocktail [100x], Fisher Scientific). Cell suspensions were shaken at 24°C, 150 rpm for 40 min. Insoluble cell debris were removed by centrifugation at 4°C, 12,000 rcf for 20 min and soluble fractions were transferred to new tubes. qPCR was performed as previously described.[1] Briefly, RNA extraction was performed using TRIzol (Fisher Scientific) and samples were treated with Dnase I (New England BioLabs) to eliminate possible DNA contamination. Quantitative PCR conditions were performed on an Applied Biosystems 7300 Real-Time PCR system using a two-step cycling protocol. The qPCR primers for CheZ forward and reverse were TTGATCCTGATGCGGTTGTG and CGCGCGATCGTTTGTACTAT, respectively. Primers were used at a final concentration of 400 nM, and 10 ng of RNA was used as template in each 20-μL reaction. Each reaction was performed in triplicate, with outlying data removed for select samples. Sixteen seconds rRNA was used as the endogenous housekeeping gene.

Total protein concentration (Pierce BCA Protein Assay, Fisher Scientific) was calculated using the microplate procedure with BugBuster-BSA (EMD Millipore) standards. Prestained ladder (Benchmark Prestained Protein Ladder, Fisher Scientific), His_6-CheZ protein, and 40 μL of boiled samples (5× SDS-dye boiled with total protein from final BugBuster step; ~175 μg total protein concentration; uniform across all experimental samples) were loaded into 12% SDS-PAGE gels (Bio-Rad). A semidry transfer apparatus (Bio-Rad) was used to transfer proteins to nitrocellulose membranes (Thermo Scientific Pierce) and blocked with 10% milk (Blotting Grade Blocker Non Fat Dry Milk, Bio-Rad; Tris-buffered saline + Tween 20 [TBS-T]) overnight at 4°C.

Western blots were performed with 1:10,000 anti-CheZ polyclonal antibody (produced by New England Peptide in rabbit) and 1:15,000 of antirabbit horse radish peroxidase antibody (Sigma Aldrich) solutions (5% BSA, TBS-T). Before incubation with anti-CheZ, it was adsorbed in 25% lysed *E. coli cheZ* knockout strain extract, 5% Bovine serum albumin (BSA, Sigma Aldrich, St. Louis, MO) to decrease nonspecific binding. Protein signal detection was performed using SuperSignal West Femto Kit (Thermo Scientific), incubated with Amersham Hyperfilm ECL (GE Healthcare) for 15 min and developed using the Konica SRX-101 (Konica Corporation).

Motility videos

E. coli containing either one or two plasmids were grown overnight, reinoculated into 5 mL of LB in 25 mL flasks, and shaken at 37°C until OD_{600} of 0.5 was achieved. Bacteria cultures were split into 1 mL subcultures in culture test tubes and induced with 0–100 μM hydrogen peroxide at 24°C, 250 rpm for 15 min. The bacteria were centrifuged at 112rcf and 4°C, washed twice, and resuspended in DPBS for brightfield motility videos (cellSense). Videos were recorded for a minimum of 100 frames for subsequent Matlab (MathWorks) analysis.[22] All videos were recorded in 8-bit greyscale using an Olympus DP72 microscope with UPLFL 20x objective lens and cellSense Standard 1.12 software (Olympus Life Science). Phase contrast (brightfield) videos were captured using 50 ms white light exposure without binning (1360 × 1024 pixel size,

319.48 nm/pixel). For data analysis, technical duplicate and biological triplicate data were obtained.

Acknowledgments

At the time this research was completed, Dr. Virgile was a doctoral research candidate at the University of Maryland, College Park. She is now a Commissioner's Fellow at the Food and Drug Administration (FDA). Partial support of this work was provided by DTRA (HDTRA1-13-0037), NSF (DMREF #1435957, ECCS#1807604, CBET#1805274), and the National Institutes of Health (R21EB024102).

Literature Cited

1. Virgile C, Hauk P, Wu HC, Shang W, Tsao CY, Payne GF, Bentley WE. Engineering bacterial motility towards hydrogen-peroxide. *PLoS One*. 2018;13(5):e0196999.
2. Zargar A, Quan DN, Emamian M, Tsao CY, Wu HC, Virgile CR, Bentley WE. Rational design of 'controller cells' to manipulate protein and phenotype expression. *Metab Eng*. 2015; 30:61–68.
3. Tsao CY, Hooshangi S, Wu HC, Valdes JJ, Bentley WE. Autonomous induction of recombinant proteins by minimally rewiring native quorum sensing regulon of *E. coli*. *Metab Eng*. 2010;12 (3):291–297.
4. Panteli JT, Forbes NS. Engineered bacteria detect spatial profiles in glucose concentration within solid tumor cell masses. *Biotechnol Bioeng*. 2016;113(11):2474–2484.
5. Forbes NS. Engineering the perfect (bacterial) cancer therapy. *Nat Rev Cancer*. 2010;10(11):785–794.
6. Forkus B, Ritter S, Vlysidis M, Geldart K, Kaznessis YN. Antimicrobial probiotics reduce *Salmonella enterica* in Turkey gastrointestinal tracts. *Sci Rep*. 2017;7:40695.
7. Borrero J, Chen Y, Dunny GM, Kaznessis YN. Modified lactic acid bacteria detect and inhibit multiresistant enterococci. *ACS Synth Biol*. 2015;4(3):299–306.
8. Mao N, Cubillos-Ruiz A, Cameron DE, Collins JJ. Probiotic strains detect and suppress cholera in mice. *Sci Transl Med*. 2018;10(445):eaao2586.
9. Wu HC, Tsao CY, Quan DN, Cheng Y, Servinsky MD, Carter KK, Jee KJ, Terrell JL, Zargar A, Rubloff GW, Payne GF, Valdes JJ, Bentley WE. Autonomous bacterial localization and gene expression based on nearby cell receptor density. *Mol Syst Biol*. 2013;9:636.
10. McKay R, Hauk P, Wu HC, Pottash AE, Shang W, Terrell J, Payne GF, Bentley WE. Controlling localization of *Escherichia coli* populations using a two-part synthetic motility circuit: an accelerator and brake. *Biotechnol Bioeng*. 2017;114(12):2883–2895.
11. Terrell JL, Payne GF, Bentley WE. Networking biofabricated systems through molecular communication. *Nanomedicine (Lond)*. 2016;11(12):1503–1506.
12. Toley BJ, Forbes NS. Motility is critical for effective distribution and accumulation of bacteria in tumor tissue. *Integr Biol (Camb)*. 2012;4(2):165–176.
13. Ravichandar JD, Bower AG, Julius AA, Collins CH. Transcriptional control of motility enables directional movement of *Escherichia coli* in a signal gradient. *Sci Rep*. 2017;7(1):8959.
14. Wei Q, Minh PN, Dotsch A, Hildebrand F, Panmanee W, Elfarash A, Schulz S, Plaisance S, Charlier D, Hassett D, Haussler S, Cornelis P. Global regulation of gene expression by OxyR in an important human opportunistic pathogen. *Nucleic Acids Res*. 2012;40(10):4320–4333.
15. Zhang A, Altuvia S, Tiwari A, Argaman L, Hengge-Aronis R, Storz G. The OxyS regulatory RNA represses rpoS translation and binds the Hfq (HF-I) protein. *EMBO J*. 1998;17(20): 6061–6068.
16. Hwang IY, Tan MH, Koh E, Ho CL, Poh CL, Chang MW. Reprogramming microbes to be pathogen-seeking killers. *ACS Synth Biol*. 2014;3(4):228–237.
17. Saeidi N, Wong CK, Lo TM, Nguyen HX, Ling H, Leong SS, Poh CL, Chang MW. Engineering microbes to sense and eradicate *Pseudomonas aeruginosa*, a human pathogen. *Mol Syst Biol*. 2011;7:521.
18. Bentley WE, Mirjalili N, Andersen DC, Davis RH, Kompala DS. Plasmid-encoded protein: the principal factor in the "metabolic burden" associated with recombinant bacteria. *Biotechnol Bioeng*. 1990;35(7):668–681.
19. DeLisa MP, Valdes JJ, Bentley WE. Quorum signaling via AI-2 communicates the "metabolic burden" associated with heterologous protein production in *Escherichia coli*. *Biotechnol Bioeng*. 2001;75(4):439–450.
20. Servinsky MD, Terrell JL, Tsao CY, Wu HC, Quan DN, Zargar A, Allen PC, Byrd CM, Sund CJ, Bentley WE. Directed assembly of a bacterial quorum. *ISME J*. 2016;10(1):158–169.
21. McKay R, Hauk P, Quan D, Bentley WE. Development of cell-based sentinels for nitric oxide: ensuring marker expression and Unimodality. *ACS Synth Biol*. 2018;7(7):1694–1701.
22. Pottash AE, McKay R, Virgile CR, Ueda H, Bentley WE. TumbleScore: run and tumble analysis for low frame-rate motility videos. *Biotechniques*. 2017;62(1):31–36.
23. Shang W, Tsao CY, Luo X, Teodoro M, McKay R, Quan DN, Wu HC, Payne GF, Bentley WE. A simple and reusable bilayer membrane-based microfluidic device for the study of gradient-mediated bacterial behaviors. *Biomicrofluidics*. 2017;11(4): 044114.
24. Alon U, Camarena L, Surette MG, Aguera y Arcas B, Liu Y, Leibler S, Stock JB. Response regulator output in bacterial chemotaxis. *EMBO J*. 1998;17(15):4238–4248.
25. Diao J, Young L, Kim S, Fogarty EA, Heilman SM, Zhou P, Shuler ML, Wu M, DeLisa MP. A three-channel microfluidic device for generating static linear gradients and its application to the quantitative analysis of bacterial chemotaxis. *Lab Chip*. 2006; 6(3):381–388.
26. Girgis HS, Liu Y, Ryu WS, Tavazoie S. A comprehensive genetic characterization of bacterial motility. *PLoS Genet*. 2007;3 (9):1644–1660.
27. Junge W. ATP synthase and other motor proteins. *Proc Natl Acad Sci U S A*. 1999;96(9):4735–4737.
28. Minamino T, Morimoto YV, Kinoshita M, Aldridge PD, Namba K. The bacterial flagellar protein export apparatus processively transports flagellar proteins even with extremely infrequent ATP hydrolysis. *Sci Rep*. 2014;4:7579.
29. Canton B, Labno A, Endy D. Refinement and standardization of synthetic biological parts and devices. *Nat Biotechnol*. 2008;26: 787–793.

Manuscript received Sep. 27, 2018, revision received Dec. 28, 2018, accepted Jan. 10, 2019.